J. Phys. Chem. A **1998,** *102,* 8946−8952

Binding of Na^+, Mg^+, and Al^+ to the *π* Faces of Naphthalene and Indole: Ab Initio Mapping Study

Robert C. Dunbar

Chemistry Department, Case Western Reserve University, Cleveland, Ohio 44106

Received: March 4, 1998; In Final Form: July 20, 1998

Binding energy maps have been calculated for the binding of Na^+, Mg^+, and Al^+ to the entire π-facial region of indole and to the parts of the naphthalene face near the long central axis. Binding sites exist for all three cations over the phenyl ring and over the pyrrole ring of indole, although for Na^+ the pyrrole site almost disappears. The phenyl binding site of indole is in all cases about 4 kcal mol^{-1} more stable than the pyrrole site and about 6 kcal mol^{-1} more stable than the similar site in naphthalene. The Hartree−Fock calculations suggested an additional stable binding site for the open-shell Mg^+ ion over the nitrogen atom of indole, but this site was not reproduced by density-functional calculations and may well be a computational artifact. A differential electrostatic picture is considered in which the π face of indole is equivalent, in its cation interactions, to the π face of naphthalene, with the addition of a differential electrostatic field equal to the difference in the electrostatic fields surrounding naphthalene and indole. The differential electrostatic picture is highly successful for Na^+, almost as successful for Al^+, and almost as successful for Mg^+. This gives quantitative support to the validity of an electrostatic approach to understanding, comparing, and predicting cation binding properties of different π-facial molecules.

Introduction

The interaction of metal ions with the π surfaces of aromatic molecules, a central and traditional concern of organometallic chemistry, is receiving a good deal of new attention. The recognition of such interactions as an important factor in determining conformations and reactions of metal-containing biologically important systems has sparked interest from a new point of view,[1,2] while the quantitative experimental study of such interactions is advancing rapidly through the exploitation of powerful new gas-phase approaches.[3−10] Especially provocative is the viewpoint, recently advocated by the Dougherty group, taking the electrostatic component of binding as pivotal in understanding variations of cation interactions with different biologically relevant π faces.[2,11,12]

Indole is an especially important model molecule for developing understanding of biologically interesting cation/π interactions, inasmuch as it is the side chain of tryptophane, and thus serves to model binding sites widely available on proteins. Moreover, it is nearly unique among the many biologically important nitrogen heterocycles in that the nitrogen is positively charged and thus is not the automatic target of an approaching cation as it is for most other molecules of this type. Accordingly, its cation/π-face interactions with cations are definitely competitive with cation/nitrogen interactions and in fact are probably predominant over the latter. Improving the understanding of the cation/π interactions of indole is thus highly relevant to thinking about where and how strongly various types of metal ions will approach, interact with, and bind to exposed tryptophane sites.

The surface properties of a molecule with respect to an approaching ionic ligand can be mapped in several informative ways, including electrostatic potential maps[11−13] and polarization maps,[14−16] giving valuable pictures of interactions with simple ions such as alkali cations. Pictures such as these based on the ion as a featureless charge become less valuable for ions with stronger interactions with the molecule, like the Mg^+ and Al^+ cations considered here. It becomes more important to map the actual binding energy to visualize the interplay of electric attraction and covalent binding that is unique for each ligand. The present work aims to develop usefully accurate binding energy maps of the π surfaces of indole and its naphthalene relative of the three title cations sitting at various positions over the π face. Calculations of the equilibrium binding energy have been reported for these molecules with alkali metals, including Na^+, at essentially the same computational level as used here.[2] The present work goes beyond these in several respects. By looking at Al^+, and particularly the open-shell ion Mg^+, stronger and more complicated interactions are addressed than the relatively weak and predominantly classical interactions of alkalis. Although not significant for the closed-shell ions, the nitrogen binding site turns out to be potentially interesting for the open-shell Mg^+ ion. Moreover, mapping the entire binding surface, rather than just the equilibrium binding site, can give insight into directions of approach toward the binding sites and the freedom the metal ion has to move around on the π face, as well as the forces acting on a metal ion not located at a binding well.

The development of the simplified potential surfaces used in molecular mechanics modeling is ultimately based on, to a large extent, more accurate quantum chemistry derived potentials. Molecular mechanics surfaces for some closed-shell cations interacting with benzene have been worked on carefully,[17] and the present calculations should offer a valuable foundation for carrying this development to the more complex surfaces of naphthalene and indole and to open-shell cations. Ultimately, it will be possible to give a similar quantum chemistry basis for modeling interactions of transition metal ions with these π faces, although these ions still present formidable computational challenges.[18] It is an ongoing goal of our group to deepen the

10.1021/jp981371t CCC: $15.00

understanding of π/cation binding for larger, more complex π surfaces and for a variety of ionic species.[8,19−22]

The shape of the metal-ion/substrate binding energy surface is important in accurate theoretical modeling of dissociation reaction kinetics involving such complexes. The semiclassical variational transition state (VTST) approach worked out by Marcus, Wardlaw, Klippenstein, and co-workers[23−25] uses the classical phase space available to the "transitional" modes (the degrees of freedom with predominant metal character in this case) in both the dissociating complex and the transition state. For a substrate like indole with multiple binding sites, it is important to know the relative energies of the different sites and the barriers between them in the assessment of the phase space volume (or density of states function) for the reactant complex. Reasonably accurate surfaces such as those undertaken here are thus an important underpinning for such high-level kinetics calculations.

The binding of these three metal ions to the benzene π face has had a reasonable amount of attention. Fairly recent theoretical studies have appeared for benzene with Na^+,[12,17,26] Mg^+,[27] and Al^+.[4,28] Experimental determinations have been reported for benzene with Na^+,[7] Mg^+,[10] and Al^+.[4] Experimental work on naphthalene and indole complexes has apparently not been reported. Mecozzi et al. reported ab initio results for Na^+ with naphthalene (28.7 kcal mol^{-1})[12] and indole (32.6 kcal mol^{-1}),[12] using a comparable basis set, that are lower than the present results by a few kcal mol^{-1}, presumably because of our making an MP2 correction for correlation and our electing not to make a correction for BSSE.

Methods

The basic set of binding energy points used Hartree−Fock (HF) calculations with the standard 6-31G* basis, carried out using the GAUSSIAN 94 quantum chemistry package.[29] The indole geometry was frozen in the fully optimized form for the isolated neutral molecule at this same HF/6-31G* level (except for points in the vicinity of the nitrogen atom, as described below). For each calculated point, the x and y position coordinates of the metal ion were chosen, and the z coordinate (the distance above the plane of the carbon framework) was optimized to give the lowest energy. For each of the three systems about 35 points on the π face were calculated, distributed to give a good characterization of the binding sites and the central saddle point and also to sample sufficiently well-dispersed points to map the overall shape of the binding surface.

About half the points were refined with the second-order Moeller−Plesset (MP2) perturbative correction for the correlation energy, still using the frozen HF geometry for indole. These MP2 points were generally chosen in the central regions of the surface, near the binding sites, and along the saddle point between them. For the points not calculated at the MP2 level, an approximate correction was applied on the basis of the extent of MP2 corrections found for the MP2 points so that the entire surface is displayed as an estimated MP2 surface. Going to the MP2 level increased the absolute binding energies by 2.5 kcal mol^{-1} (Na^+), 7.8 kcal mol^{-1} (Mg^+), and 12.5 kcal mol^{-1} (Al^+). It also decreased the distance of the metal ion from the plane by about 0.1 Å. However, the MP2 correction was reasonably constant over the π face and made little difference to the relative depths of the binding wells, the height of the central barrier, or the general shape of the surface. For Na^+, going from HF to MP2 changed the shape of the binding surface by less than 0.5 kcal mol^{-1}. For Mg^+ the largest change in relative energies of different points was less than 1 kcal mol^{-1}, while for Al^+, the largest change was on the order of 1.5 kcal mol^{-1}. The largest relative MP2 corrections were for peripheral points vs central points; the MP2 corrections to the surface shape in the binding valleys were much less than these values.

Although the main calculations were done with a frozen indole geometry, the effect of allowing geometry relaxation was explored by a number of calculations at the HF level using full optimization of all variables except for the x/y position of the metal ion. For Na^+ and Al^+, the relaxation energy was around 1 kcal mol^{-1} in the central regions of the surface and somewhat greater, up to around 2 kcal mol^{-1}, around the periphery (metal ion sitting over the carbons). For Mg^+, the relaxation energies tended to be somewhat greater than these, perhaps by a factor of 1.5. Although these relaxation effects are insignificant compared with the uncertainties in the overall binding energy, they do change the shape of the binding surface noticeably, and accordingly, approximate relaxation corrections were applied to all the points on the calculated surfaces. As discussed below in detail, relaxation energies were much larger when the metal ion was near the nitrogen atom, probably reflecting rehybridization effects with attendant significant changes in geometry.

Basis set superposition errors (BSSE) are not negligible in these systems. Some counterpoise trials indicated that the total BSSE is on the order of 2 kcal mol^{-1} for the HF calculations and 5 kcal mol^{-1} for the MP2 calculations for the Mg^+/indole and Al^+/indole systems and smaller for Na^+/indole. It might be appropriate to lower the calculated binding energies by amounts of this order. However, the best approaches to BSSE corrections, and even whether they are appropriate at all, are controversial and open questions.[30] We can hope, encouraged by Bauschlicher,[27] that calculations such as these with small basis sets may show useful cancellation of errors from BSSE and from basis set incompleteness, and the resulting binding energies may be more accurate than might be suggested by the counterpoise calculation of BSSE. The present point of view is that we are not primarily interested in calculating accurate absolute binding energies. BSSE effects should be reasonably constant across the π face and should not seriously affect the shape of the calculated binding surface. Similarly, comparing different metal ions and different neutral ligands should have validity even in the face of substantial uncertainty in the absolute numbers arising from the relatively small basis set. On the basis of these considerations, no BSSE corrections were made.

No corrections were made for differential zero-point energy (ZPE) effects. These have been found to be small, at least for Mg^+/benzene.[27] To confirm this for the present systems, representative calculations were done on the Al^+/indole system. Full geometry optimization and vibrational frequency calculations were carried out at the HF level for the two binding minima (phenyl-ring site and pyrrole-ring site). The increase of ZPE between indole and the Al^+ complex was such that the binding energy would be decreased by 1.1 kcal mol^{-1} by a ZPE correction. More important for the present purpose, the ZPE correction was found to be the same within 0.1 kcal mol^{-1} for the two binding sites, suggesting that ZPE effects should have no significant effect on the shapes of the binding energy surfaces. In the same way, differential heat capacity and entropy effects are such that the enthalpy and free energy of complexation might be altered by amounts on the order of 1 kcal mol^{-1} upon warming to 300 K, but such effects are very similar for the two binding sites and should have no significant effect on the shapes of the binding surfaces.

The binding energy surface was constructed from the calculated set of points using the three-dimensional fitting and

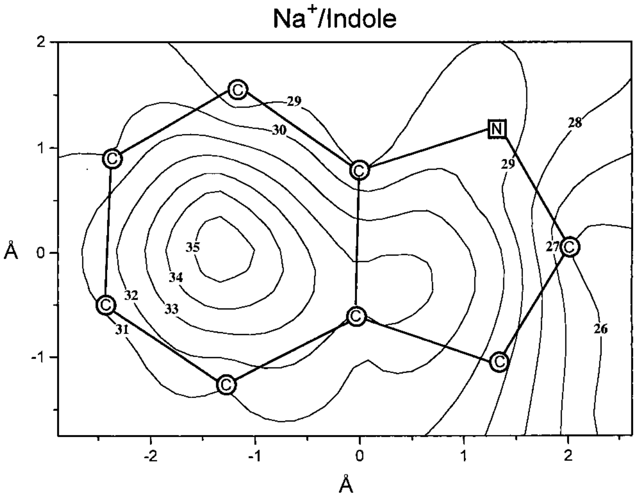

Figure 1. Contour map of the binding energy of Na^+ to the indole surface. At each point on the surface, the binding energy value represents the binding energy (kcal mol^{-1}, referenced to separated species) at the optimum value along the *z* (vertical) axis. The energies were only sampled as far out as the carbon−nitrogen periphery so that values and contours outside the indicated peripheral boundary have no meaning (except for a small region around the nitrogen atom). Most sampled points were calculated with the indole geometry frozen in the shape of neutral indole, with corrections for geometry relaxation effects as discussed in the text.

smoothing algorithm contained in the Origin data-processing package.[31] Since no points were calculated outside the carbon−nitrogen perimeter of the indole skeleton, no attention should be paid to energy values outside this perimeter, even though the fitting program extends the displayed equal-energy contours farther out.

Naphthalene complexes were calculated in a similar way to indole complexes, on the basis of the frozen HF geometry, with corrections for correlation and geometry relaxation. The π face was not fully mapped for these systems, but the shape of the surface is certainly very similar to the phenyl side of indole. Points were calculated along the long (*x*) axis, using a sufficient set of *y* values to cover the parts of the π face needed to compare with the binding valley floor of indole. The *z* (out-of-plane) coordinate was as usual optimized at each point to give the lowest energy.

Additional calculations were made at two points for Mg^+/indole using density functional theory and a somewhat improved basis to compare the pyrrole-ring binding site with the possible nitrogen binding site. The B3LYP hybrid functional as available in GAUSSIAN 94 was used,[29,32] and the basis consisted of the same 6-31G* set described above, augmented by a set of four diffuse functions on the nitrogen. At the pyrrole binding site, full geometry relaxation and optimization were carried out, yielding a stable local minimum point. No local minimum was found for metal-ion binding to the nitrogen, so a calculation was carried out in which the Mg atom was constrained to lie above the nitrogen atom, making a 90° angle to the ring plane with respect to displacement in the *y* (short axis) direction, while all other variables were fully optimized.

Most calculations were done on a local IBM RS/6000 model 3AT computer. Some were done on the Silicon Graphics Power Challenge computer at the Ohio Supercomputer Center.

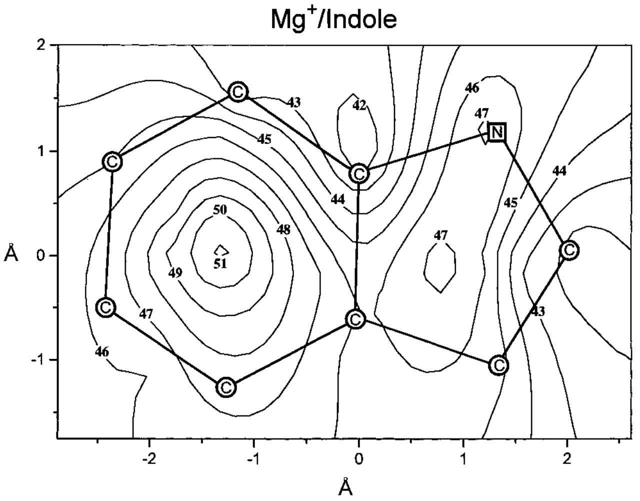

Figure 2. Binding energy surface for Mg^+/indole, similar to Figure 1.

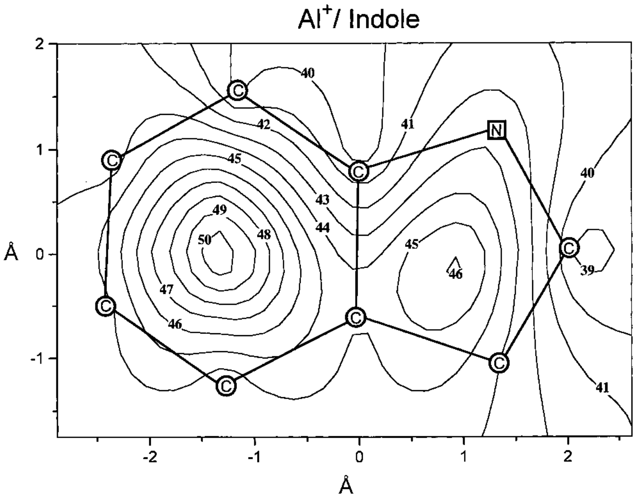

Figure 3. Binding energy surface for Al^+/indole, similar to Figure 1.

TABLE 1: Calculated Binding Energies at Various Sites (kcal mol^{-1})

	Na^+	Mg^+	Al^+
phenyl site/benzene	29.5 (28.0[a])	41	39 (35[b])
phenyl site/naphthalene	31(30[c])	45	43 (39[c])
phenyl site/indole	36 (35[c])	51	50 (46[c])
pyrrole site/indole	~32	47	46
saddle point/naphthalene	29	41	38
saddle point/indole	~32	46	43

[a] Experiment, from ref 7. [b] Experiment, from ref 4. [c] Best estimated absolute binding energy based on the experimental benzene number.

Results and Discussion

***π* Face.** Figures 1−3 display the binding surfaces to indole for the three metal ions. These contour plots show contours of equal binding energy, remembering that the metal ion/π plane distance is optimized at each point on the surface. The surfaces show well-defined binding wells in the central region of each of the two rings. Table 1 summarizes the key features of the surfaces, giving the binding energies for the two wells, as well as the energy of the saddle point forming the barrier between the two wells. It is well-known that the binding site on the phenyl ring is more stable than that on the pyrrole ring, as is clearly reflected by the figures and Table 1. Mg^+ may have an additional binding site over the nitrogen atom, which is discussed below.

Table 2 shows the equilibrium metal-ion/aromatic plane distances for various metal/π face binding sites (MP2 level).

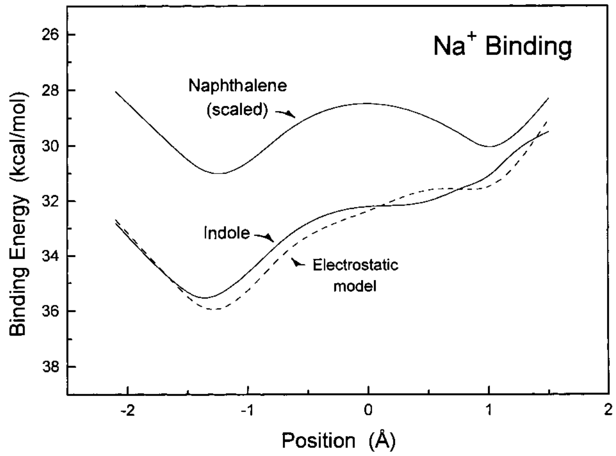

Figure 4. Binding energy profiles for Na^+ along the molecular long axis, following a path along the floor of the binding valley on the indole surface. The curve shown for indole corresponds to the valley floor along the horizontal axis of Figure 1. The naphthalene curve follows the corresponding path along the naphthalene π face. The "electrostatic model" curve is constructed as described in the text, considering indole binding to be equivalent to naphthalene binding corrected by the difference in electrostatic fields of the two molecules.

TABLE 2: Binding Distances (Å) between the Molecular Plane and the Metal Ion

	Na^+	Mg^+	Al^+
phenyl site/benzene	2.40	2.25	2.32
phenyl site/naphthalene	2.37	2.24	2.27
phenyl site/indole	2.39	2.20	2.25
pyrrole site/indole	~2.47	2.27	2.30
saddle point/naphthalene	2.48	2.34	2.37
saddle point/indole	~2.47	2.30	2.35

Not surprisingly, there is a strong correlation between binding distance and binding energy for a given metal ion on different sites.

It is useful to compare binding to indole with that to other simple π faces. Table 1 facilitates comparison with other simple π faces by giving binding energies, calculated at the same computational level, for the benzene and naphthalene faces. In terms of comparing the different metals, Mg^+ and Al^+ have similar binding energy to the aromatic faces of benzene and naphthalene, while binding of Na^+ is about 12 kcal mol^{-1} weaker. This pattern is almost exactly preserved for binding of these metal ions to the phenyl site of indole and similarly to the pyrrole site of indole.

We can take the view (expanded below) that indole is closely equivalent to a naphthalene with an embedded additional electric field of basically dipolar character. Figures 4−6 compare the binding profiles of these two substrates. (The odd-appearing asymmetrical potential curve for naphthalene, denoted "scaled" on the figures, is explained in detail below; briefly, the coordinates have been distorted to allow for the geometry difference between naphthalene and indole.) The binding energies to indole in the vicinity of the pyrrole binding well are only 1 or 2 kcal mol^{-1} stronger than those to naphthalene, but the relative binding energy of indole increases quite steadily toward the phenyl end. The straightforward interpretation is that the positive charge accumulation in the nitrogen region tilts the electrostatic potential surface quite uniformly downward toward the phenyl end of the indole molecule. The binding to the phenyl well of indole is 5−7 kcal mol^{-1} stronger than that to naphthalene. That these differences are largely electrostatic is strongly indicated by the observation that they are quite similar for all three metal ions, as well as by the agreement with the differential electrostatic model.

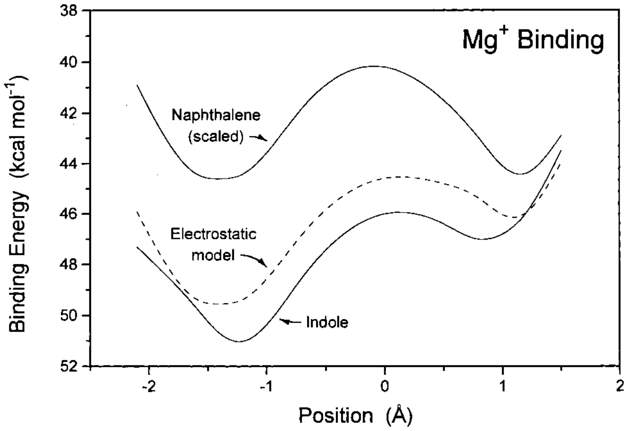

Figure 5. Binding energy profiles for Mg^+, similar to Figure 4.

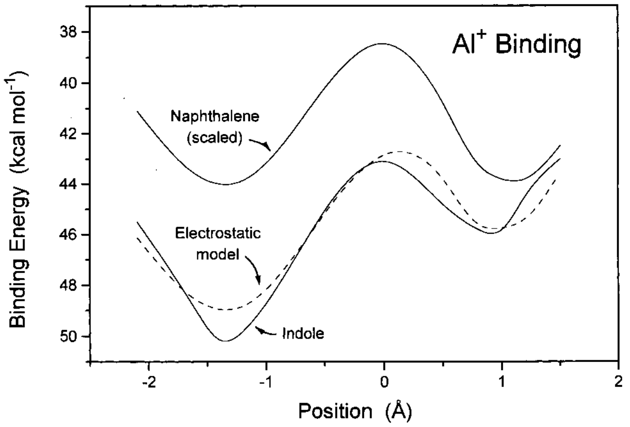

Figure 6. Binding energy profiles for Al^+, similar to Figure 4.

For these metal ions, the barrier to passage across the saddle point between the two π-face binding wells is not very high (either for indole or for naphthalene), being only a small fraction of the total binding energy. Other than the fact that the dipole field of indole strongly tilts the binding potential surface downward toward the phenyl site, going from naphthalene to indole seems to have little effect on the character of the barrier. Thus, if we look at the average of the barriers to crossing from either of the two binding sites on indole to the other, this average barrier is equal to the barrier to site-to-site crossing on naphthalene (for each metal ion). A result of the electrostatic tilt of the indole binding surface is that the pyrrole site offers little stability for any of these ions—even for the best-case Al^+ ion, it costs only 3 kcal mol^{-1} in activation energy for the ion to leave the pyrrole site and cross into the phenyl site.

Tetrahedral Nitrogen Binding Site. It is a reasonable possibility that the nitrogen of indole might rehybridize from sp^2 to sp^3 and take on tetrahedral character, with the metal ion coordinating to the nitrogen lone pair. To explore this possibility, the metal ion was moved out along the path leading toward a fully tetrahedral nitrogen geometry while allowing the indole geometry to relax. Geometry relaxation is essential in this process. It was found that moving a metal ion out to a position approximately on top of the nitrogen was hopelessly unfavorable using the frozen indole geometry (much more unfavorable than the corresponding positions over carbon atoms). Allowing the nitrogen-bound H to bend out of plane by 20 or 30°, with no other geometry relaxation, gave complexes of more reasonable energy. However, allowing full geometry relaxation with the metal ion over the nitrogen produced a large additional energy gain, since the conformation around the nitrogen adjusted to reflect a substantial degree of rehybridization. The binding energies indicated in the vicinity of the nitrogen in Figures 1−3 correspond to these fully optimized structures.

As indicated by Figures 1 and 3, the Na^+ and Al^+ ions did not show anything like a stable "tetrahedral" nitrogen binding site. The fully optimized structures with the metal ion moving outward toward a tetrahedral geometry around the nitrogen were more favorable than similar optimized geometries placing the metal ion in comparable positions relative to a carbon atom. However, moving the metal ion away from the pyrrole π binding site toward the nitrogen, and beyond the nitrogen toward a truly tetrahedral conformation, was strongly and continuously uphill for these metals. There was no indication of a favorable geometry or a local energy minimum near a true tetrahedral nitrogen conformation. These features are quite clearly displayed by Figures 1 and 3.

On the other hand, the open-shell Mg^+ ion showed a well-defined "tetrahedral" nitrogen site based on results at the level of full HF geometry optimization. As shown in Figure 2, placing the Mg^+ ion directly over the nitrogen gives a binding energy well virtually equal in depth to the pyrrole π-facial site. This nitrogen binding site is a shallow local minimum, with the metal ion located 2.24 Å above the nitrogen and C−N−Mg angles close to 90°. The nitrogen-bound hydrogen bends down to give an H−N−Mg angle of 128°. The two carbon−nitrogen bonds lengthen from 1.37 to 1.42 Å, indicating that the nitrogen atom has lost a good deal of its original sp^2 character. It is not favorable to move the metal ion farther out beyond the nitrogen to a more nearly tetrahedral-nitrogen conformation.

Since this nitrogen site for Mg^+ was in such surprising contrast to the otherwise similar Al^+ results, it was suspected that it might be an artifact of the HF calculations. To get a cross-check on this possibility, density functional (DFT) calculations were carried out on the two points corresponding to pyrrole-site binding and nitrogen-site binding of Mg^+. The pyrrole site was reproduced by this approach, with a binding energy of 42 kcal mol^{-1} (compared with 47 kcal mol^{-1} from the MP2 calculation). However, the nitrogen binding site was not reproduced. Similar to the Al^+ surface, moving Mg^+ from the pyrrole site to the nitrogen site was found to be uphill by several kcal mol^{-1}. Placing the metal ion directly over the nitrogen atom gave the same reyhbridization and bond-length changes as were found using HF, but this structure was 3.1 kcal mol^{-1} higher in energy than the pyrrole binding site. Thus, the DFT results suggest that the Mg^+ binding surface is quite similar to the Al^+ surface shown in Figure 3 in this respect and do not support the suggestion of a well-defined nitrogen binding site for the open-shell Mg^+ ion. Given the contradictory answers to this question obtained from the two alternative theoretical approaches at the levels that were feasible in this work, the possibility of favorable nitrogen-site binding for open-shell ions in pyrrole and indole will have to be resolved by higher-level calculations.

Role of Electrostatic Binding. There is confusion in the literature over the description of a portion of the binding in systems such as this as "electrostatic." Bauschlicher's group, for instance, has used this term to refer to the classical interaction energy of the ion, considered to be a unit point charge, with the charge distribution of the polarized molecule.[27,33] It thus includes both charge-permanent-multipole and charge-induced-multipole interactions. From this point of view Bauschlicher and Partridge can state, for instance, that for Mg^+/benzene "the bonding is electrostatic in origin, principally charge induced-dipole...".[27] On the other hand, in what is probably the more usual convention (see ref 30), Dougherty's group[11] uses the term "electrostatic" to denote the interaction of the charge with the electrostatic field of the *unpolarized* molecule, thus omitting charge-induced-multipole (polarization) interactions. This is a convenient definition, since it is this energy that is mapped by the electrostatic-field mapping algorithms of computational packages such as GAUSSIAN 94. We will arbitrarily adopt this latter definition (no polarization) in using the word "electrostatic interaction" in the present paper. From this point of view, as Dougherty's group has recognized, the binding of cations to π faces is *not* primarily "electrostatic", since the polarization interactions (particularly the charge-induced-dipole interaction) are strong. In fact, even for Na^+, which is a case with an especially large proportion of electrostatic binding, almost half of the binding energy to indole is due to polarization and other nonelectrostatic contributions. For the indole binding cases examined here, the electrostatic components of binding at the phenyl site are 20, 22, and 21 kcal mol^{-1} for Na^+, Mg^+ and Al^+, respectively, compared with total binding energies (Table 1) of 36, 50, and 51 kcal mol^{-1}, respectively. (Incidentally, presuming that the Na^+ case represents a good approximation to pure electrostatic-plus-polarization binding, it is clear the both Mg^+ and Al^+ have substantial components of covalent or dative binding; calculation shows that only about 4 kcal mol^{-1} of their additional binding energies relative to Na^+ can be attributed, through electrostatic-plus-polarization interactions, to the fact that they sit ∼0.15 Å closer to the ring than Na^+.)

However, *differential* electrostatic effects are highly effective in accounting for the differences in cation binding between π faces of different molecules, and it is in this way that Dougherty's group has drawn conclusions from calculated electrostatic binding fields.[1,2,12] It is particularly interesting to use the present quantitative binding surfaces to test the assumptions underlying the use of electrostatic potentials to predict binding variations among different molecules. Specifically, we can test the hypothesis that the difference between binding to indole and binding to naphthalene is accounted for by differential electrostatic potential effects. Indole is a highly dipolar molecule, with a large concentration of positive charge near the nitrogen, compared with the lack of dipolar character of naphthalene, but in other ways these π faces are quite similar, so this is an especially appealing case for quantitative testing of these effects. In this picture, the polarization, charge-transfer, covalent, and other nonelectrostatic contributions to ion binding will be envisioned as being the same for the two neutrals.

This comparison is straightforward in principle. The electrostatic potential fields of the unperturbed naphthalene and indole neutrals are readily calculated from the ab initio wave functions, and the difference between them is taken at each point of interest to give the differential electrostatic field. The values of this field taken at the ion bonding distances, when added to the naphthalene binding energy values, are expected to yield numbers equal to the corresponding indole binding energies at the corresponding ion positions.

There are two complications to bear in mind in carrying this out. First, the corresponding energies being subtracted must all be taken at identical points in space. In these comparisons, points were considered at various positions along the x axis (the long axis of the molecules), and at each x value the y and z values were taken to be those corresponding to the bottom of the indole binding valley. This was not a significant consideration at the phenyl end, since, as suggested by Figures 1−3 and Table 2, there is not a significant difference in the binding positions between indole and naphthalene at this end of the molecules; points along the central symmetry line of naphthalene correspond well enough to matching points along the indole binding valley. However, around the saddle point and at the pyrrole end the binding positions for indole deviate significantly from the central axis that corresponds to the naphthalene binding positions (as seen in Figures 1−3). Thus, the points evaluated in those regions are quite a bit away from the central axis of naphthalene and do not correspond to the bottom of the naphthalene binding valley. This was addressed by choosing points lying along the indole binding valley and using the computed naphthalene binding energies at the corresponding naphthalene positions. This raises the affected naphthalene points in Figures 4−6, with a maximum correction (at the saddle points) of about 1 kcal mol^{-1}.

The other complication to making useful point-by-point comparisons at the pyrrole end is that the phenyl ring is about 20% larger than the pyrrole ring. Thus, at the pyrrole end the geometric center of the indole ring is displaced from the center of the corresponding naphthalene ring. Since the binding minima tend to be close to the centers of the rings, this will give a displacement of the pyrrole binding site of indole from the corresponding site of naphthalene, which would make nonsense of the attempt to compare corresponding binding sites if the points were simply compared at equal x positions. As a convenient way to make the comparisons meaningful, we scaled the x values of the right-hand side (positive x values) of the naphthalene molecule down by 20%. This is indicated in Figures 4−6 by denoting the naphthalene binding curves as “scaled”. Thus, if it is desired to read the naphthalene binding energy of a metal ion at a true x position on the right-hand side of naphthalene in one of these figures, the indicated x position should be multiplied by 1.25. This scaling adjustment results in the approximate coincidence of the positions of the indole and naphthalene binding wells on the right-hand side of the figures.

The results of these comparisons are shown in Figures 4−6. If the hypothesis is correct that indole is equivalent to naphthalene with an added differential electrostatic field, we expect the curves for “electrostatic model” and “indole” to coincide exactly. It is seen that for Na^+ this expectation is borne out with remarkable success. For Al^+ the correspondence is nearly as good, and for Mg^+ it is just slightly less good. For Al^+ the differential electrostatic model underestimates the binding energy at the phenyl site by around 1 kcal mol^{-1}, a discrepancy that has doubtful significance within the various uncertainties, but succeeds well over most of the surface. For Mg^+ the model is off by 1−1.5 kcal mol^{-1} over much of the surface, which is again a discrepancy of doubtful significance. Mg^+ is on its face a poor choice for application of this simple picture, first, because it is an ion of high electron recombination energy (favoring charge-transfer binding effects) and, second, because it has an open-shell ($3s^1$) valence configuration that might readily take on p character and polarize the singly occupied orbital (as Bauschlicher finds to be the case for Mg^+ binding to several ligands.[27]) The simple electrostatic picture based on a unit spherical charge at the position of the metal atom could be upset both by charge-transfer effects and by distortion of the Mg^+ valence electron cloud. Thus, it is particularly interesting that this simple picture performs so well for Mg^+.

It will be interesting in future work to see if this picture holds up as well for transition metals. There is hope that it may do so, since the idea that the polarization, dative, and covalent contributions to bonding will be invariant between naphthalene and indole seems likely to hold up well for all metal ions, and additivity of the different contributions to bonding is at least a reasonable expectation.

Binding Energies. The present calculations are far from an ab initio computational level that would produce believable absolute binding energies. However, by comparison of the calculated values to corresponding values for benzene calculated at the same level of theory, it should be possible to make good estimates of the indole and naphthalene binding energies by reference to the benzene values, which are at least potentially easier to obtain by accurate experiments or high-level calculations. The benzene binding energies are given in Table 1 and calculated in the same way as for indole and naphthalene (HF/6-31G*, with corrections for MP2 estimates of correlation and for geometry relaxation at the HF level). Whatever values one chooses to assign to the benzene binding energies, it should be valid to assign quite good values for naphthalene and indole by adding to them the increments suggested by Table 1.

For Na^+/benzene, a recent experimental value of 28.0 kcal mol^{-1} is also given in Table 1.[7] This is an equilibrium-based number worthy of confidence and is in acceptable accord with the present calculation.

For Mg^+/benzene the only experimental value of benzene binding is an upper limit of 27 kcal mol^{-1} from photodissociation.[10] The method used in this latter work, while apparently careful, is not yet established as reliable; it gave binding energies for Ag^+ ions to several ligands that were suprisingly much lower than values from other approaches.[8] So this upper limit cannot be regarded as definitive. Bauschlicher’s[27] ab initio value of 30.4 kcal mol^{-1} (which he judges to be 3−5 kcal mol^{-1} lower than the true value) was derived from calculations at a somewhat higher level than the present work but still not high enough to give real confidence. The present results, particularly the MP2 corrected value, are larger than Bauschlicher’s, probably owing in part to our not making any correction for BSSE, and we would suspect that the present Mg^+/benzene number in Table 1 may be too high in absolute value. Overall, the Mg^+ binding thermochemistry does not seem sufficiently certain to warrant assigning absolute values at this time beyond saying that it has order-of-magnitude similarity to Al^+.

For Al^+ binding to benzene, a recent experimental study by radiative association kinetics[4] considered the available values for the binding energy and assigned a best value of 35 kcal mol^{-1}. Ab initio values,[4,28] including the present one, are a few kcal mol^{-1} higher than this, but no really large and convincing calculation has been reported. Because of the neglect of BSSE, the present calculated value can be expected to err on the high side.

Conclusions

The ion binding site of indole is clearly the phenyl π site for all three of these metal ions; this site is more favorable than the pyrrole site by about 4 kcal mol^{-1} for all three cases. When the metal ion is over the nitrogen atom, rehybridization and possible development of a “tetrahedral” nitrogen site are observed, but this site is several kcal mol^{-1} less stable than the pyrrole binding site for Na^+ and Al^+; its stability is uncertain in the Mg^+ case, but we are inclined to believe the DFT result showing that it is several kcal mol^{-1} less stable than the pyrrole site in this case as well. This site needs to be further examined for its possible importance in binding more electronically flexible metal ions such as the transition elements.

The absolute binding energies given here are not very reliable, and errors of 20% in absolute values would not be surprising. Factors contributing to this uncertainty are the relatively small basis sets and low level of theory used, neglect of BSSE, and neglect of ZPE effects. Comparing the three metal ions with one other should be considerably more accurate, since many of the sources of error are common to all three sets of calculations. Most accurate should be the comparison of different points on one binding energy map, since we were quite careful to consider the effects that are likely to vary from one point to another. We expect the contours of any one of the maps of Figures 1−3 to be reliable relative to each other to better than 1 kcal mol^{-1}.

Except for the possible differences near the nitrogen, the binding surfaces for Mg^+ and Al^+ with indole are quite similar. For Na^+, the binding is weaker by about 15 kcal mol^{-1} and the pyrrole-site binding well essentially disappears.

The tilt of the binding potential surface created by the internal dipolar electric field of indole has as one consequence the fact that binding to the phenyl site of indole is 4−6 kcal mol^{-1} stronger than binding to naphthalene. Another consequence is to destabilize the pyrrole site such that the activation energy for the metal ion to cross to the phenyl site is always low for indole.

It is an excellent approximation to consider that metal ion binding to indole is equivalent to binding of the same metal to naphthalene, enhanced by a superimposed differential electrostatic interaction corresponding to the ion sitting in the polar electric field of the indole molecule. For the closed-shell ion Na^+, this is valid to a high degree of accuracy. This equivalence is almost as good for Al^+ and almost as good for Mg^+. The excellent success of this extremely simple model gives quantitative support to the use of simple electrostatic approaches to predict the binding energy differences between different π faces.

Acknowledgment. The support of the donors of the Petroleum Research Fund, administered by the American Chemical Society, is gratefully acknowledged, as is the provision of computational support by the Ohio Supercomputer Center. Professor Stephen Klippenstein has been generous with sharing his knowledge, expertise, and computer resources, all of which were invaluable for this project.

References and Notes

(1) Dougherty, D. A. *Science* **1996**, *271*, 163.

(2) Ma, J. C.; Dougherty, D. A. *Chem. Rev.* **1997**, *97*, 1303.

(3) Cerda, B. A.; Wesdemiotis, C. *J. Am. Chem. Soc.* **1995**, *117*, 9734.

(4) Dunbar, R. C.; Klippenstein, S. J.; Hrušák, J.; Stöckigt, D.; Schwarz, H. *J. Am. Chem. Soc.* **1996**, *118*, 5277.

(5) Crestoni, M. E.; Fornarini, S. *Organometallics* **1996**, *15*, 5695.

(6) Freiser, B. S. *J. Mass Spectrom.* **1996**, *31*, 703.

(7) Guo, B. C.; Purnell, J. W.; Castleman, A. W. J. *Chem. Phys. Lett.* **1990**, *168*, 155.

(8) Ho, Y.-P.; Yang, Y.-C.; Klippenstein, S. J.; Dunbar, R. C. *J. Phys. Chem. A* **1997**, *101*, 3338.

(9) Meyer, F.; Khan, F. A.; Armentrout, P. B. *J. Am. Chem. Soc.* **1995**, *117*, 9740.

(10) Willey, K. F.; Yeh, C. S.; Robbins, D. L.; Duncan, M. A. *J. Phys. Chem.* **1992**, *96*, 9106.

(11) Mecozzi, S., Jr.; West, A. P.; Dougherty, D. A. *Proc. Natl. Acad. Sci. U.S.A.* **1996**, *93*, 10566.

(12) Mecozzi, S.; West, A. P. J.; Dougherty, D. A. *J. Am. Chem. Soc.* **1996**, *118*, 2307.

(13) *Chemical Applications of Atomic and Molecular Electrostatic Potentials*; Politzer, P., Truhlar, D. G., Eds.; Plenum: New York, 1981.

(14) Bohm, G. *Biophys. Chem.* **1996**, *59*, 1.

(15) Alkorta, I.; Perez, J. J.; Villar, H. O. *J. Mol. Graphics* **1994**, 3.

(16) Alkorta, I.; Perez, J. J. *Int. J. Quantum Chem.* **1996**, *57*, 123.

(17) Caldwell, J. W.; Kollman, P. A. *J. Am. Chem. Soc.* **1995**, *117*, 4177.

(18) Hoyau, S.; Ohanessian, G. *J. Am. Chem. Soc.* **1997**, *119*, 2016.

(19) Lin, C.-Y.; Dunbar, R. C. *Organometallics* **1997**, *16*, 2691.

(20) Pozniak, B. P.; Dunbar, R. C. *J. Am. Chem. Soc.* **1997**, *119*, 10439−10445.

(21) Dunbar, R. C.; Faulk, J. D. *Chem. Phys. Lett.* **1993**, *214*, 5.

(22) Dunbar, R. C.; Uechi, G. T.; Solooki, D.; Tessier, C. A.; Youngs, W.; Asamoto, B. *J. Am. Chem. Soc.* **1993**, *115*, 12477.

(23) Klippenstein, S. J. *J. Chem. Phys.* **1992**, *96*, 367.

(24) Klippenstein, S. J. *J. Chem. Phys.* **1991**, *94*, 6469.

(25) Klippenstein, S. J. *Chem. Phys. Lett.* **1990**, *170*, 71.

(26) Kumpf, R. A.; Dougherty, D. A. *Science* **1993**, *261*, 1708.

(27) Bauschlicher, C. W. J.; Partridge, H. *Chem. Phys. Lett.* **1991**, *181*, 129.

(28) Stöckigt, D.; Hrušák, J.; Schwarz, H. *Int. J. Mass Spectrom. Ion Processes* **1994**, *149/150*, 1.

(29) Frisch, M. J.; Trucks, G. W.; Schlegel, H. B.; Gill, P. M. W.; Johnson, B. G.; Robb, M. A.; Cheeseman, J. R.; Keith, T. A.; Petersson, G. A.; Montgomery, J. A.; Raghavachari, K.; Al-Laham, M. A.; Zakrzewski, V. G.; Ortiz, J. V.; Foresman, J. B.; Cioslowski, J.; Stefanov, B. B.; Nanyakkara, A.; Challacombe, M.; Peng, C. Y.; Ayala, P. Y.; Chen, W.; Wong, M. W.; Andres, J. L.; Replogle, E. S.; Gomperts, R.; Martin, R. L.; Fox, D. J.; Binkley, J. S.; Defrees, D. J.; Baker, J.; Stewart, J. J. P.; Head-Gordon, M.; Gonzalez, C.; Pople, J. A. *GAUSSIAN 94*; Gaussian, Inc.: Pittsburgh, PA, 1995.

(30) Stone, A. J. *The Theory of Intermolecular Forces*; Oxford University Press: Oxford, 1995.

(31) *Microcal Origin3D*, version 3.5; Microcal Software, Inc.: Northampton, MA, 1991−1994.

(32) Becke, A. D. *J. Chem. Phys.* **1993**, *98*, 5648.

(33) Bauschlicher, C. W. J.; Partridge, H.; Langhoff, S. R. *J. Phys. Chem.* **1992**, *96*, 3273.